Photometric observation of defunct satellites using small telescopes: preliminary results

A Rachman[1], T Djamaluddin[1] and A Vananti[2]

[1] Research Center for Space, National Research and Innovation Agency (BRIN), Indonesia
[2] Astronomical Institute of University of Bern (AIUB), Switzerland

Email: abdr001@brin.go.id

Abstract. Detailed information on space debris characteristics is essential, among other things, to mitigate its hazards to operational satellites and people on Earth. One can perform photometric observations to get some of this information. The light curve data obtained from the observations can be analysed to identify the space debris attitude in orbit. While usually people use at least 50 cm telescopes for this purpose, smaller telescopes still have the potential. With this in mind, we have configured a system, located at Tilong Science Center in Indonesia, using less than 30 cm telescopes for photometric observations and obtained some preliminary results. We have compared the results with light curves from the same objects in the AIUB light curve database maintained by the Astronomical Institute of the University of Bern in Switzerland. In the case of defunct GLONASS satellites, as a sample, our limited result shows consistency with the reference. Our system with 20 cm reflector can reveal similar light curve morphology to the ones in the AIUB database for relatively bright objects (magnitude less than 14). Typically, four peaks appear in a phase diagram of decommissioned GLONASS satellites which resemble their four sides. On the other hand, our smaller system with 10 cm refractor, can only be used to get the inferred periods for relatively bright objects. This result, while only preliminary, is inspiring considering that the primary telescope objectives of our system are only 20 cm in maximum compared to the reference database, which uses a 1-m telescope.

1. Introduction

The risk from space debris keeps growing as their number continues to propagate. According to the Space-track website[3] (www.space-track.org), there are currently more than 25,000 resident space objects, most of them debris, circling the Earth with sizes larger than 10 cm. In the last three years, we witnessed a dramatic increase in the number of low Earth objects (Figure 1). The figure shows a remarkable increase of artificial space objects tracked by the Space Surveillance Network[4] in the last 20 years. The increase from 2000 to 2010 was dominated by fragments generated from the FENGYUN-1C antisatellite test conducted by China in 2007 and the accidental collision between the defunct COSMOS 2251 and the operational IRIDIUM 33 spacecraft in 2009. The increase from 2010 to 2020 was driven by the initial build-up of the STARLINK large constellation (120 STARLINK spacecraft were launched from May to November 2019) and by the proliferation of CubeSats below about 650 km altitude. The increase from 2020 to 2022 continues to be driven by the STARLINK and CubeSats below about 650 km altitude, with a new increase near 1200 km altitude driven by the OneWeb large constellation [1].

---

[3] The website is owned by the United States Department of Defense and publicly available for registered users.

[4] The space surveillance network (SSN) is a combination of optical and radar sensors used to support the US Joint Space Operations Center's (JSpOC) mission to detect, track, identify, and catalog all manmade objects orbiting the earth.
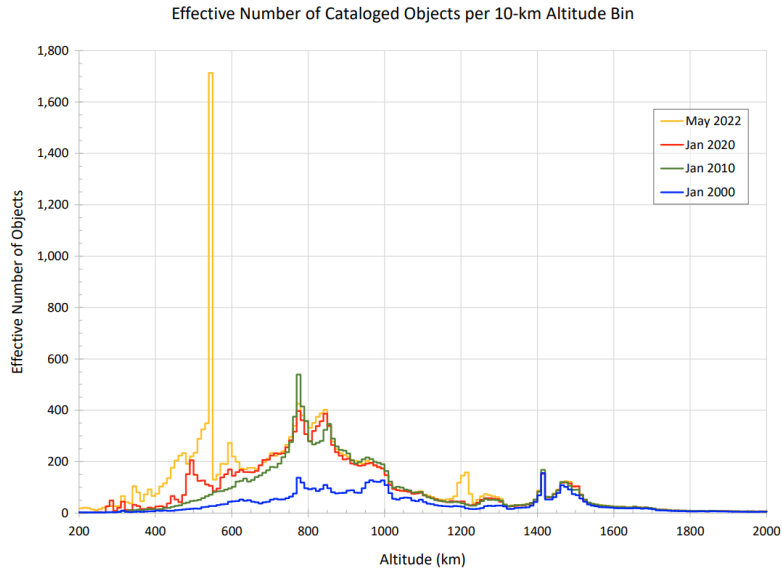
Figure 1. Effective numbers of objects per 10 km altitude bin between 200 and 2000 km altitude at four different epochs [1].

Many experts believe that the solution for space debris issue requires not only prevention but also remediation to stabilize the population. The latter, which is also called active debris removal (ADR), is performed by nudging large debris into a safer orbit or forcing them to reenter the atmosphere prematurely. For the ADR mission to be successful, sufficient knowledge about the attitude of the space debris is mandatory. One method to obtain this is by performing photometric observations using optical telescopes to get the light curves of the space debris. Routine and careful observations, followed by light curve analysis, can reveal temporal evolution of the attitude properties, such as rotational periods (or the equivalent rotational rates). The light curve analysis can also benefit in mitigating the risk of reentering space objects. Similar procedures have long been used for natural objects such as comet and meteor.

Usually, telescope systems used for photometric observations of satellites and space debris have larger than 50 cm primary objectives. This will guarantee that the systems can observe very dim targets with a large enough signal-to-noise ratio (SNR) to allow for accurate analysis. However, smaller telescopes still have the potential to be utilized for the same purpose. With this in mind, we used two small telescopes installed at Tilong Science Center, a station owned by the National Research and Innovation Agency of Indonesia (BRIN) and acts as a supporting facility for Timau National Observatory of Indonesia. Dio et al. [2] have used one of the telescopes for the purpose of detection, identification, and initial orbit determination of GEO satellites. This paper will describe how we use the small telescopes for photometric observations to get light curves of space debris. Then, how we evaluate the result by comparing it with a reference database.

2. The system

Our current setup consists of a GSO 8-inch Ritchey-Chretien reflecting telescope with 203 mm objective and 1625 mm focal length to give an f/8 focal ratio. The detector is an SBIG STF-8300M CCD with 3326×2504 px of resolution and 5.4 µm pixel size. The combination of the optical system and the detector gives a field of view of 38×29 arcmin and 0.69 arcsec/px of image scale. The system is equipped with a color filter wheel with several filters including Bessel photometric filters. The telescope, the imaging train, and all the attached accessories, which weigh no more than 15 kg, sit nicely on a Paramount MyT mount (left side of Figure 2). The mount is a robotic German equatorial mount with $6°/s$ of maximum slew speed and is put on a tripod. The CCD and the filter wheel are controlled using MaxIm DL software, while the mount is controlled using TheSkyX Pro software which comes with it and is produced by the same company (Software Bisque). The system is located inside a 16ft Astro Haven clamshell dome which stands about 3 meters above the ground (right side of Figure 2). The station's coordinate is $10° 8' 31'' \text{S}, 123° 43'54''\text{E}$, at about 100 m above sea level. In addition, we used a Takahashi FSQ 106 ED refractor as the second OTA. The OTA has a 106 mm objective and 530 mm focal length to give an f/5 focal ratio. The combination of the second OTA with the detector gives a field of view of 116×88 arcmin and 2.10 arcsec/px of image scale. We call the first and the second OTA as GSO OTA and FSQ OTA, respectively.

Figure 2. The telescope system used in this work (left) and its enclosure (right).
The second OTA is shown in the inset on the left image.

To track a resident space object (RSO), the system relies on the ability of TheSkyX to slew the telescope to the target, and track it through its *Track Satellites* button on the *Telescope* window. If the satellite is currently above the horizon, the mount is slewed to intercept the satellite's path then the mount's tracking rates are set to match the satellite's rates. If the satellite is currently below the horizon, TheSkyX waits until it is above the horizon then begins the *slew and track satellite* process. To correct any error in the tracking due to mechanical errors of the system and uncertainty in the satellite orbital data, users can interact with the system by providing it with the amount of tracking offsets that will be applied to the mount's position. We used the standard satellite tracking feature which comes with TheSkyX Pro and not the Advanced Satellite Tracking module which is an add-on. Figure 3 illustrates an example of initial and final condition of satellite tracking process using the satellite tracking feature in TheSkyX Pro. Optimal tracking is achieved when the satellite is centered in the field (represented by a red box). Mechanical errors and uncertainty in the satellite orbital data may cause the satellite to fall away from the center. To adjust the position of the satellite, we click inside the region away from the satellite's current position. The green X shows this new offset, and, when the correct offset is applied, the satellite will slowly move to the center of the field.
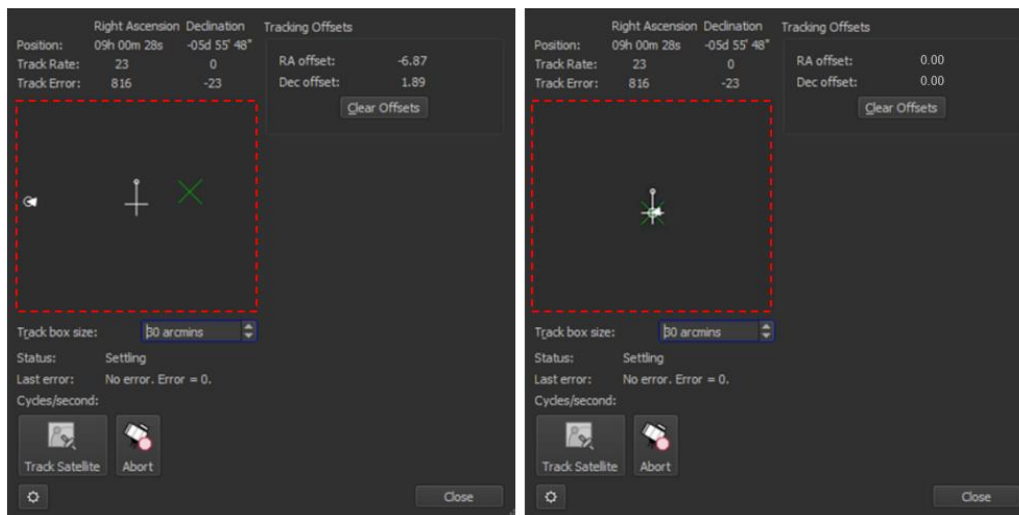
Figure 3. The satellite tracking control in TheSkyX Pro at the initial condition (left) and at the final condition (right). The region inside the red box represents the background sky. The white circle represents the satellite, the white arrow drawn through this circle shows the magnitude of the satellite's tracking rate and its current trajectory. The gray crosshairs show the center of the field. The green X represents the current Tracking Offset that is applied to the mount's position.

Currently, there is no automated pipeline for the system yet. The orbital data is taken from Space-track website (www.space-track.org) in the form of two-line element (TLE) data which is downloaded manually before the observing time. Network Time Protocol (NTP) is used for computer time synchronization. The collected data is stored in the same computer for the data acquisition which is a laptop running on Windows 10 with 8 GB of RAM. The data series in FITS format is processed manually using the multi-aperture photometry tool in AstroImageJ software to produce preliminary light curve plots and measurement data. The measurement data is later processed using a MATLAB script to obtain the final light curve plots. Afterward, we used the Phase-diagram Reconstruction Method (PRM) from AIUB [5] to find the apparent (synodic) period and the corresponding phase diagram. The method basically works by iteratively folding a light curve using a range of period values to get a phase diagram with minimum dispersion which corresponds to the inferred period. Thus, PRM produces two outputs: the inferred period and the phase diagram.

3. Test, evaluation, and outlook
The effectiveness of the system was tested during several clear nights from March until April 2022. For this purpose, several decommissioned GLONASS satellites were selected. The selection is based on the availability of the objects in the AIUB light curve database maintained by the Astronomical Institute of the University of Bern in Switzerland [3]. The data for the database, which will be called the reference database in this study, is obtained using a 1-meter reflecting telescope named ZIMLAT situated at the Swiss Optical Ground Station and Geodynamics Observatory Zimmerwald. This approach allows us to compare the resulting light curves from this study and the light curves from the same objects in the reference database. Many objects in the database including decommissioned GLONASS satellites have been observed for several years, therefore, allowing researchers to study their attitude state evolution [4]. The selected defunct GLONASS satellites in this study are the objects in the database that belong to a special group of rotating objects called oscillating rotators.

During data acquisitions, we normally use 1 sec exposure time to optimize frame rates which gives around 0.6 frames per second. As expected, the most difficult part of the test is to get images with sufficient SNR due to the small size of the telescope's primary objectives. To deal with the problem, we always do sub-framing (manually) while trying to put the target near the center of the frame to optimize the CCD read-out time. The size of the sub-frames is usually less than 200×200 px. We also normally set the CCD to 2×2 binning to increase its sensitivity and cool it down to $-13°C$. On all occasions, no filter was used and no image calibration was performed. We found that most of the time, it is necessary to repeat *the slew and track satellite* process one or two times at the beginning of the acquisition to speed up the automatic process of putting the target at the center of the frame. Interfering with the system by giving it some tracking offsets usually is not necessary.

Nineteen light curves from 14 different objects were obtained from the observations. To make the comparison with the reference database, we manually searched within the database which light curve from the same satellite shows a (roughly) similar pattern of phase diagram to our result. This is necessary since phase diagrams of one object usually vary from time to time. The result of the comparison indicates that the GSO OTA can produce light curves with similar morphology to the ones in the reference database for relatively bright objects (magnitude less than 14). Typically, four peaks appear in a phase diagram of decommissioned GLONASS satellites which resemble the "four sides" of the satellites, and most of the time they come in two pairs [6]. While the SNR in our result is generally much lower than the ones in the database especially due to the much smaller telescope's primary objectives, our system can roughly produce similar light curve patterns in its result. The FSQ OTA can only be used to get the inferred periods for relatively bright objects.

We will describe three cases to represent the result. The first case is the comparison between our light curve and the reference for COSMOS 2141 satellite (Figure 4). Our light curve was obtained using 1 sec exposure time similar to the reference using the GSO OTA. Using the system configuration and the brightness of the object then, we managed to get an average SNR of 14. We can see from the figure that despite the higher SNR of the reference light curve, the similarity of the patterns between both light curves is obvious. Figure 5 shows the corresponding phase diagrams of the light curves which were obtained using PRM. The inferred periods of our light curve and the reference are 177.00 sec and 184.17 sec, respectively. Again, we see the similarity between the patterns of the phase diagrams despite the phase difference. Four sharp peaks which come in two pairs (one is significantly narrower than the other) are clearly seen. The fact that the period can be accurately measured using PRM, indicates that the object was rotating uniformly around its axis of rotation during the acquisition time. The period can even be estimated visually by inspecting the pattern in the light curve.
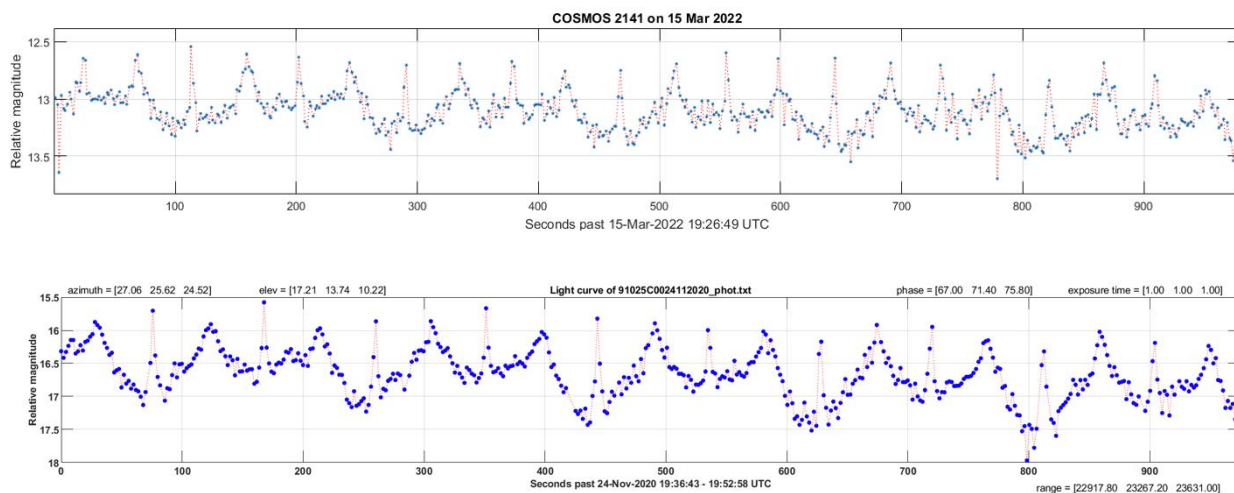
Figure 4. The comparison between the light curves for case 1 produced by this study (top) and the one from the AIUB database (bottom).
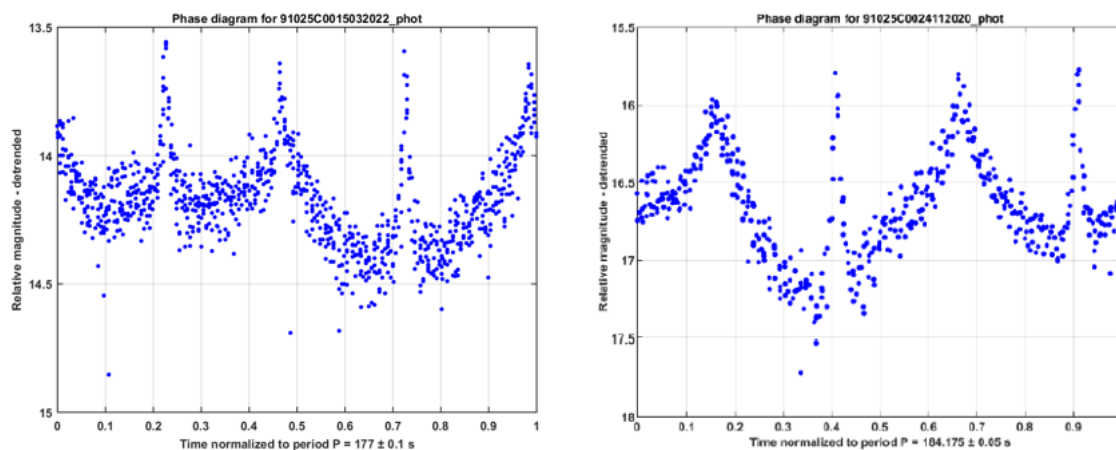
Figure 5. Phase diagrams of the light curves for case 1 produced by this study (left) and the one from the AIUB database (right).

The second case is the comparison between our light curve and the reference for COSMOS 2307 satellite (Figure 6). Our light curve was obtained using 2 sec exposure time using the FSQ OTA as opposed to 1 sec used by the reference. The 2 seconds exposure time allowed us to get an average SNR of 13. The data were acquired in three series which explains the gap in the light curve. Again, we can see from the figure that despite the higher SNR of the reference light curve, the similarity of the patterns between both light curves is obvious. The phase diagram is also obtained using PRM (Figure 7). The inferred periods of our light curve and the reference are 69.85 sec and 74.45 sec, respectively. However, it is not easy to see the similarity between the patterns of the phase diagrams due to the low quality of our light curve. Nevertheless, assuming that we have a similar pattern with the reference phase diagram, we can see that there are more than four peaks and it is not easy to see any pairing. Therefore, the light curve is not a typical light curve of defunct GLONASS satellites. The fact that the inferred period can still be accurately measured using PRM, indicates that the object was rotating uniformly around its axis of rotation during the acquisition time, similar to the case one.
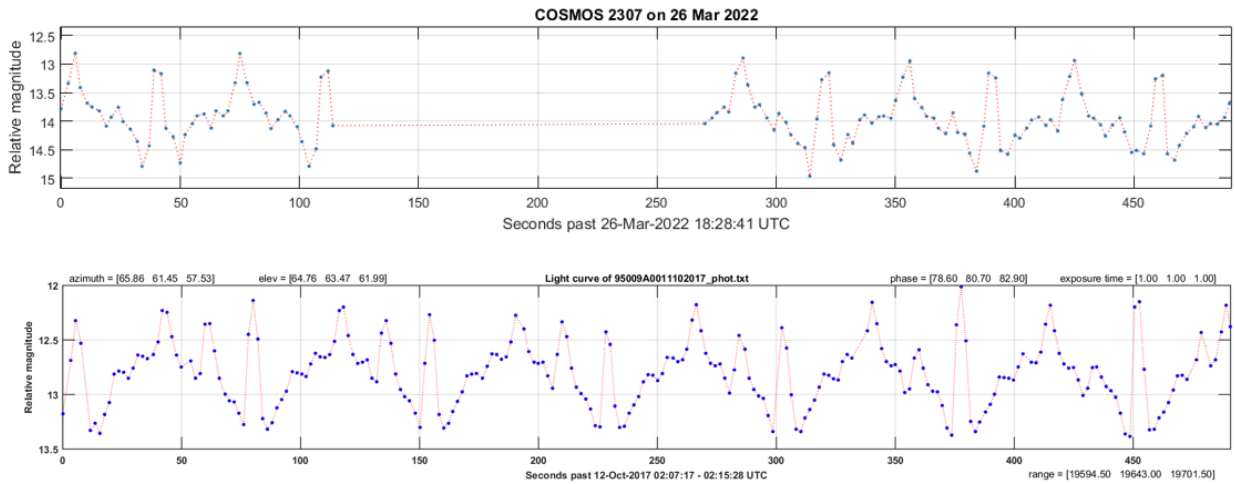
Figure 6. The comparison between the light curves for case 2 produced by this study (top) and the one from the AIUB database (bottom). A large data gap appears in the top light curve.
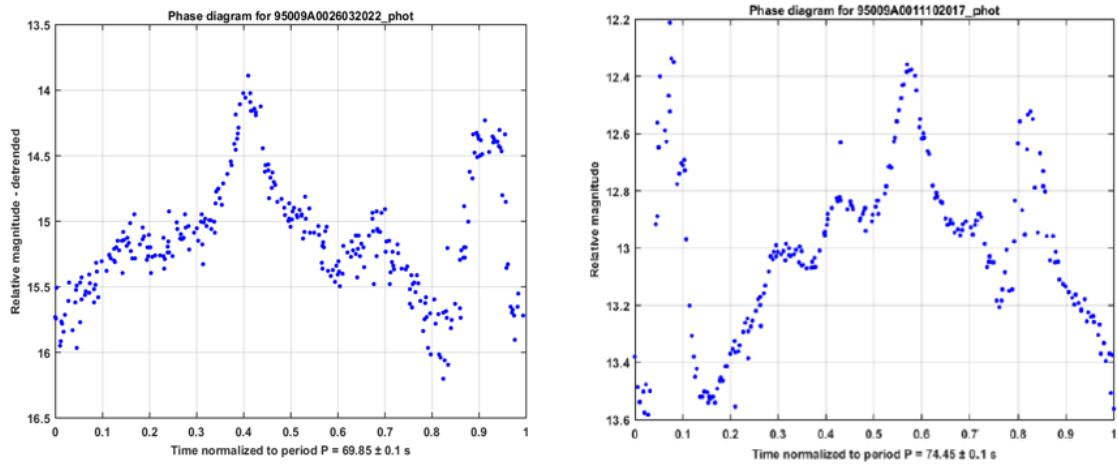
Figure 7. Phase diagrams of the light curves for case 2 produced by this study (left) and the one from the AIUB database (right).

The third case is the comparison between our light curve and the reference for COSMOS 2395 satellite (Figure 8). Our light curve was obtained using 1 sec exposure time similar to the reference using the FSQ OTA. With this exposure time, the system can only yield an average SNR of only 5. Nevertheless, we can still vaguely see from the figure, the similarity of the patterns between both light curves. The phase diagram is also obtained using PRM (Figure 9). The inferred periods of our light curve and the reference are 84.37 sec and 99.25 sec, respectively. However, it is difficult to see the similarity between the patterns of the phase diagrams due to the low quality of our light curve. Nevertheless, assuming that we have a similar pattern with the reference phase diagram, we still have four peaks which come in two pairs (one is significantly higher than the other). Therefore, we can presume that the light curve is still a typical light curve of defunct GLONASS satellites. The fact that the inferred period can still be accurately measured using PRM, indicates that the object was rotating uniformly around its axis of rotation during the acquisition time, similar to the previous cases.
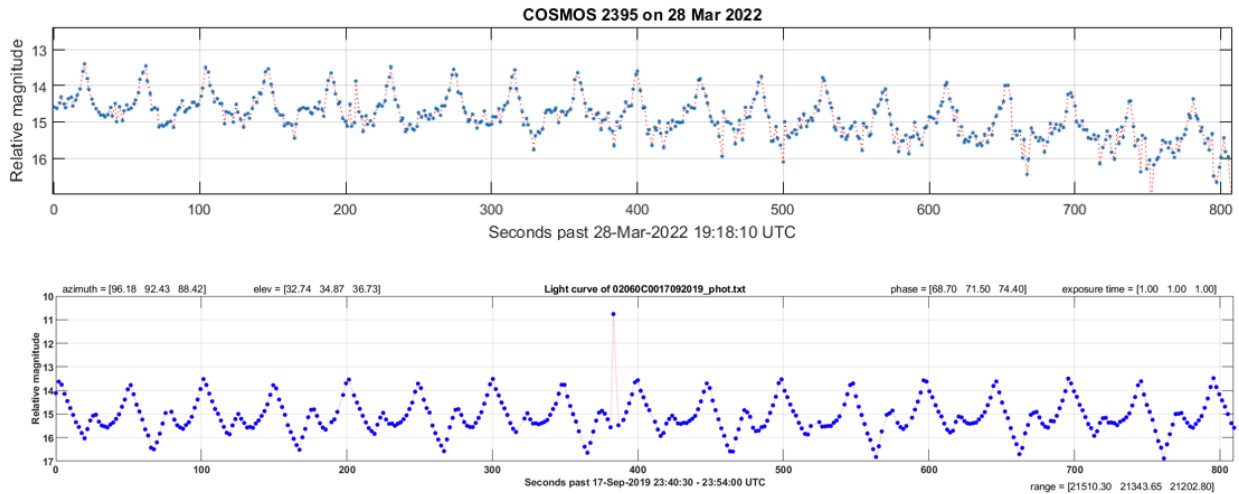
Figure 8. The comparison between the light curves for case 3 produced by this study (top) and the one from the AIUB database (bottom).
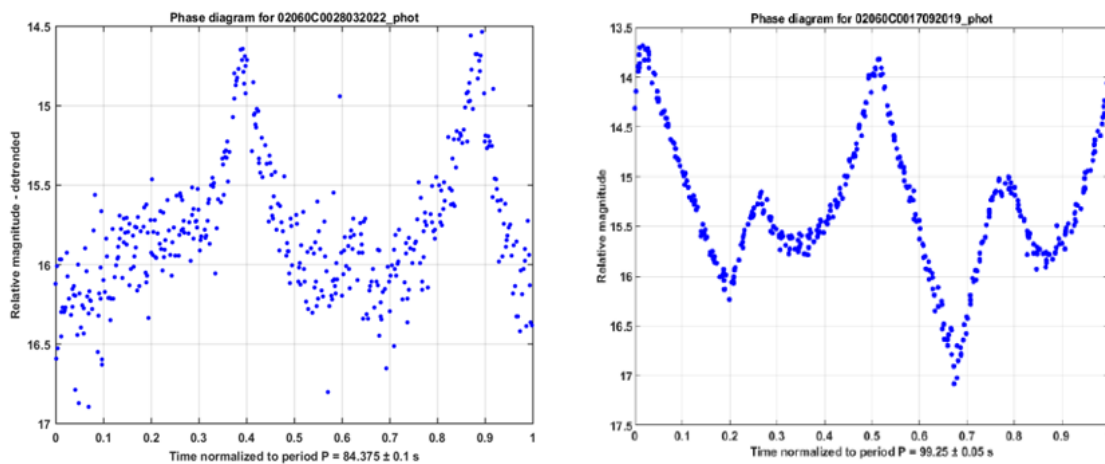
Figure 9. Phase diagrams of the light curves for case 3 produced by this study (left) and the one from the AIUB database (right).

Physically, a quasi-periodic light curve indicates uniformly rotating debris around their axis of rotation during the acquisition time. This we have seen in all the three cases described above. On the contrary, a complex light curve whose period is very difficult to get using PRM (if not impossible) indicate a tumbling space debris likely due to collision or other disturbances. Basically, the attitude of a satellite after decommissioned (or any kind of uncontrolled spacecraft) is completely governed by internal or external torques and this could result in any kind of attitude mode during data acquisitions. However, it is expected theoretically that eventually any uncontrolled spacecraft will most likely rotate around its major principal axis (the axis corresponding to the largest principal moment of inertia) after it met a condition called *flat spin* [7, p. 501]. Looking back at our three cases, this is what we believe has occurred to the associated satellites considering that they all retired decades ago: COSMOS 2141 in February 1992, COSMOS 2307 in September 1999, and COSMOS 2395 in November 2007.

To summarize, we have given an evident that small telescopes can significantly contribute to space situational awareness through photometric observations of relatively bright satellites and space debris. This is an inspiring result considering that the primary telescope objectives of our system are only 20 cm in maximum compared to the reference database, which uses a 1-m telescope. The procedure described in this paper can serve as a basic procedure for the bigger 50 cm robotic telescope also available at the station. Furthermore, considering that small telescopes are available in many places in Indonesia now, we hope that this study will motivate their use in the realm of space situational awareness which becomes more and more important nowadays.

4. Conclusion

Light curve analysis can be used to identify space debris attitude in orbit. One can utilize small telescopes to obtain the data by means of photometric observations. With this in mind, we have configured a system, located at Tilong Science Center in Indonesia, using less than 30 cm telescopes for photometric observations and obtained some preliminary results. We have compared the results with light curves from the same objects in the AIUB light curve database maintained by the Astronomical Institute of the University of Bern in Switzerland. In the case of defunct GLONASS satellites, our limited result shows consistency with the reference. To be specific, our system with 20 cm reflector can reveal similar light curve morphology to the ones in the AIUB database for relatively bright objects (magnitude less than 14). On the other hand, our smaller system with 10 cm refractor, can only be used to get the inferred periods for relatively bright objects. This preliminary result is inspiring given that the primary telescope objectives of our system are only 20 cm in maximum compared to the reference database, which uses a 1-m telescope. We believe that the procedure described in this paper can serve as a basic procedure for the bigger 50 cm robotic telescope also available at the station. Furthermore, we hope this result will encourage Indonesian people to use their small telescopes in the realm of space situational awareness.

References

[1]   NASA ODPO 2022 Effective number of cataloged objects per 10-km altitude bin *Orbital Debris Quarterly News* **26** Issue 2

[2]   Danarianto M D, Maharani A M, Falah B M and Rohmah F 2022 *Proc. The Int. Symp. on Space Science (Indonesia)* (IOP Publishing)

[3]   Šilha J, Schildknecht T, Pittet J N, Rachman A and Hamara M 2017 *Proc. 7th European Conf. on Space Debris (Darmstadt)* (ESA Space Debris Office)

[4]   Rachman A, Schildknecht T, Šilha J, Pittet J N and Vananti A 2017 *Proc. 68th Int. Astronautical Congress (Adelaide)*

[5]   Šilha J, Pittet J N, Hamara M and Schildknecht T 2018 *Advances in Space Research* **61** 844–61

[6]   Rachman A, Schildknecht T and Vananti A 2018 *Proc. 69th Int. Astronautical Congress (Bremen)*

[7]   Wertz J R 1978 *Spacecraft attitude determination and control* (Dordrecht/Boston/London: Kluwer Academic Publishers)